Wave-equation deconvolution: A short-period demultiple tool for streamer, OBN and land environments

Gordon Poole[1*], Milad Farshad[1], Zhaoyu Jin[1] and Brandon Li[1], discuss a multiple prediction approach analogous to higher-dimensional gapped deconvolution, whereby the deconvolution operator is expressed in the image domain instead of the time domain.

Introduction

Many surface-related multiple prediction approaches, such as SRME (Berkhout and Verschuur, 1997), predict multiples by convolving data with multiple generators in the space-time domain. These multiple generators should be recorded as primary arrivals with sufficiently small reflection angles, as well as having well-sampled offsets in the x and y directions. For most modern 3D acquisition geometries, these conditions are typically met for long-period multiple generators coming from the deeper section. In this case, the surface-consistent convolutions forming the heart of the SRME method are good enough to produce an accurate multiple prediction.

For shallow water or land datasets, short-period reverberations dominate the multiple content, generating a curtain of multiples following every primary reflection. These short-period multiples relate to source- and receiver-side peg-leg multiples generated by strong reflecting interfaces in the shallow section. As these reflections have not been recorded well enough at small reflection angles, the SRME approach often breaks down. A popular alternative is model-based water layer demultiple (MWD), in which a Green's function representing the water layer reflection is used as a proxy for the primary arrival (Wang et al., 2011). MWD has proven to be very effective at attenuating water bottom peg-leg multiples but is not practical for predicting multiple reverberations corresponding to other more localized shallow reflectors, such as shallow gas or channel features.

Deconvolution-based approaches offer an attractive alternative, whereby the periodicity of multiple reverberations within the data itself are used to derive a multiple prediction operator (Biersteker, 2001). However, deconvolution-based approaches are sensitive to shot and receiver sampling, and in many cases are not suitable for 3D implementations.

So far, we have discussed demultiple approaches based on the summation of surface-consistent convolutions to predict multiples. An analogous set of methods, based on wave-equation extrapolation, has been described by Pica et al. (2005). Instead of convolving data with primary reflections at the surface, this approach forward-extrapolates input gathers down into an image of the primary reflectors. This forward-extrapolated data is multiplied by the image at each image depth to create a reflecting wavefield. Finally, the reflecting wavefield is forward-extrapolated to the surface to produce the multiple estimate. If a known multiple generator has not been sufficiently well imaged, for example the water bottom reflection, a spiky horizon-like event may be inserted into the reflectivity as a substitute (Wiggins, 1988).

In this paper we discuss a multiple prediction approach analogous to higher-dimensional gapped deconvolution, whereby the deconvolution operator is expressed in the image domain instead of the time domain (Poole, 2019).

Method

Equation 1 defines the wave-equation multiple modelling approach described by Pica et al. (2005) as a linear equation. The three multiple modelling steps outlined in this linear equation are also illustrated in Figure 1. In Step (a), each frequency, f, in the input data is forward-extrapolated to every location (coordinates x,y,z) in the subsurface, populating the values in matrix D_Φ. This forward-extrapolation step requires knowledge of the shallow velocities and uses a one-way extrapolation engine (Biondi, 2006). In Step (b), the forward-extrapolated wavefield is multiplied by the reflectivity image, r, to create a reflecting wavefield. Then in Step (c), the reflecting wavefield is forward-extrapolated
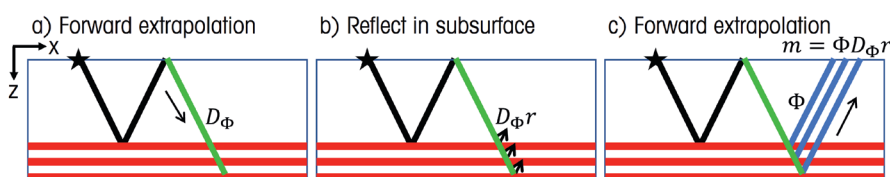

Figure 1 Illustration of the three steps involved in wave-equation multiple modelling. Step a) Forward-extrapolate input data to each depth step in the subsurface. Step b) Create the reflecting wavefield by multiplying the forward-extrapolated wavefield by the reflectivity. Step c) Forward-extrapolate the reflecting wavefield to the surface.

back to the surface using the extrapolation operator, Φ. Finally, the resulting wavefield is inverse Fourier-transformed from the temporal frequency domain (f) to the time domain (t) using operator F^{-1}. If the reflectivity is known, we may use this strategy to model multiples.

$$m(t,x,y) = F^{-1} \, \Phi(f,x,y,z) \, D_\Phi \, (f,x,y,z) r(x,y,z) \qquad (1)$$

Equation 2 uses the multiple modelling equation to define a cost function, ε, based on the sum-of-squares difference between the recorded data, d, and the modelled multiples. The optimal reflectivity image, r, responsible for minimising the error may be found by iterative inversion methods, such as steepest descent or conjugate gradients.

$$\varepsilon(r) = [d(t,x,y) - F^{-1} \, \Phi(f,x,y,z) \, D_\Phi \, (f,x,y,z) r(x,y,z)]^2 \qquad (2)$$

A minimum depth for the reflectivity image prevents the trivial solution of a unit spike at zero depth. The minimum depth is analogous to the gap in gapped deconvolution. A sufficiently large time range of input data must be used to make the process statistically reliable and prevent the approach from damaging primaries.

Once the optimal reflectivity image has been derived, the multiple prediction may be made by applying the linear operators in Equation 1. Finally, adaptive subtraction may optionally be used to subtract the multiple prediction from the input data.

In summary, the proposed approach consists of two steps. The first step involves solving an optimization problem to derive the optimal reflectivity image responsible for predicting multiples from input data using wave-equation multiple modelling. The second step uses the reflectivity image for wave-equation multiple prediction. The two steps are analogous to the two steps involved in gapped deconvolution, namely operator design followed by operator convolution. We call the method wave-equation deconvolution, or WEDecon for short.

Data examples

The first data example comes from a 20,000 km² towed-streamer acquisition from the North Viking Graben area of the Norwegian North Sea. The acquisition deployed a triple-source setup recorded by 12 multi-sensor streamers with a 100 m separation. Prior to demultiple, the input data underwent swell noise attenuation followed by joint source designature with source- and receiver-deghosting. Finally, the resulting data were redatumed to the free surface. Figure 2a shows a stack section of the input data, the main short-period multiple generators consisting of the water bottom and shallow gas reflectors. Figures 2b and 2c show MWD water bottom multiple predictions from the source- and receiver-sides respectively. We can see how the source-side prediction has a bias for diffraction tails dipping to the bottom right, and the receiver-side prediction has a bias for diffraction tails dipping to the bottom left. Based on this observation, and following Cooper et al. (2015), it is necessary to use both source- and receiver-side predictions to accurately model the multiples in this data. It is
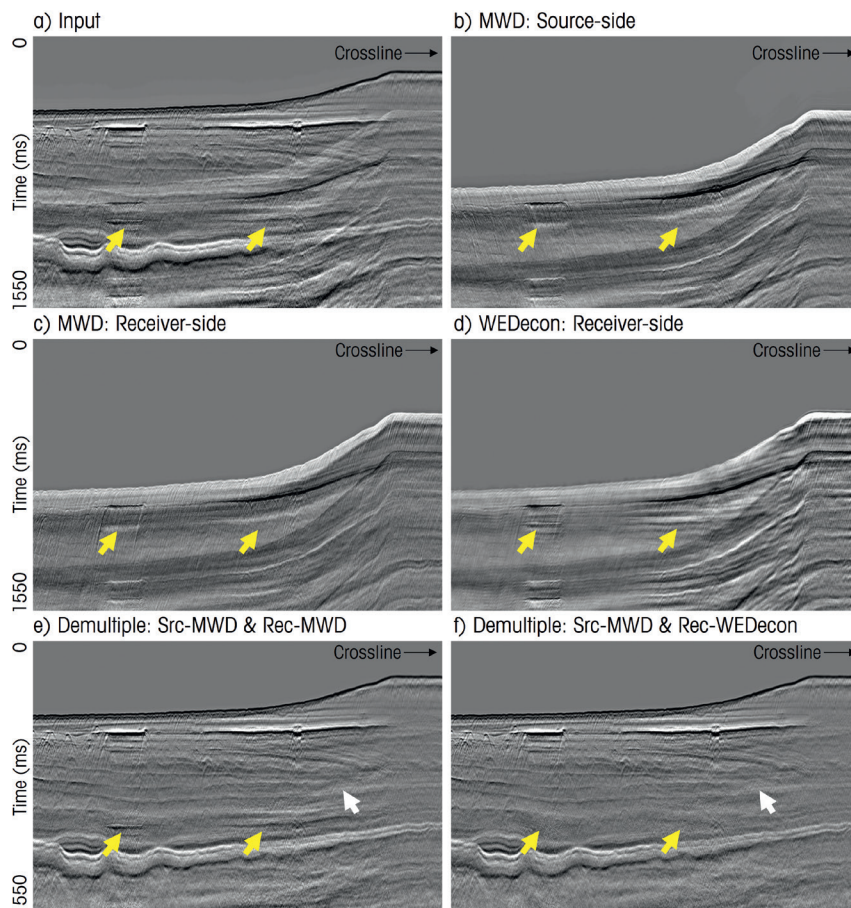

Figure 2 Stack sections comparing: a) Input data before demultiple, b) Source-side MWD multiple prediction, c) Receiver-side MWD multiple prediction, d) WEDecon multiple prediction, e) Demultiple using source- and receiver-side MWD multiple predictions, and f) Demultiple using source-side MWD and receiver-side WEDecon multiple predictions.
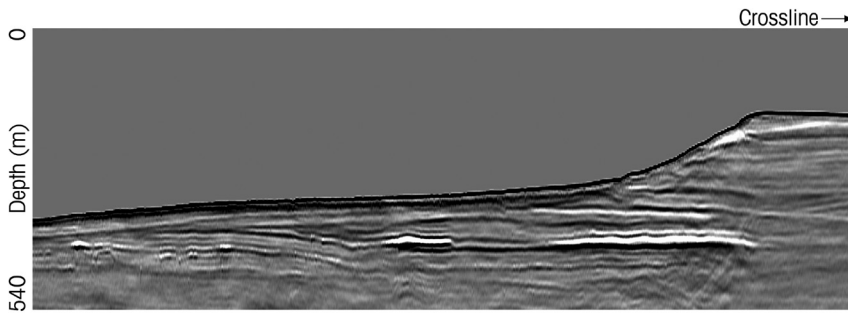
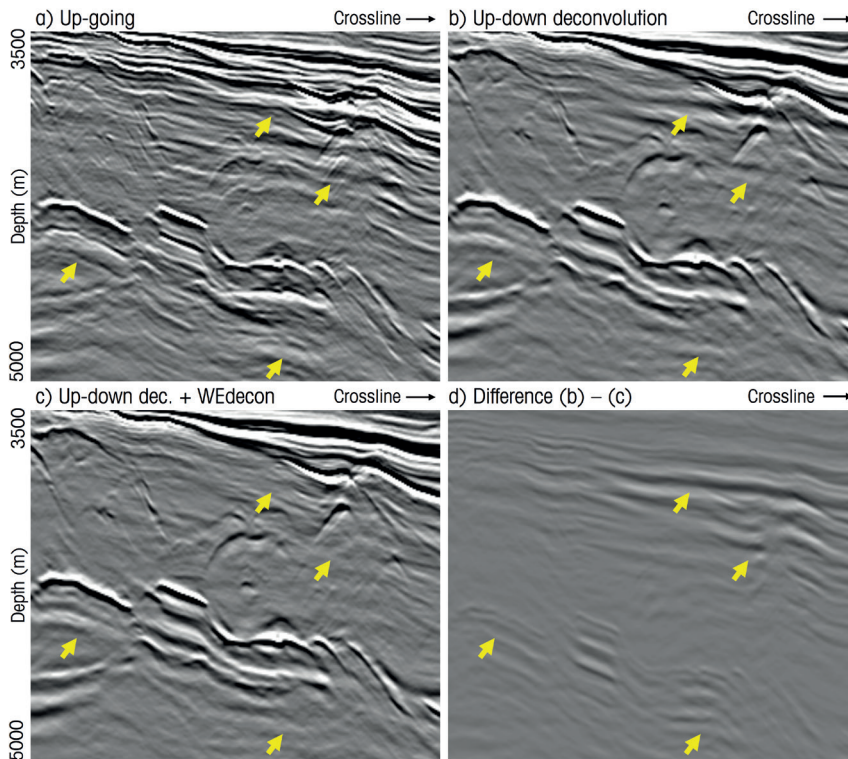**Figure 3** WEDecon reflectivity image, inline view.

Figure 4 Deep RTM inline sections for: a) Up-going data, b) Data after up-down deconvolution, c) Data after cascaded application of up-down deconvolution and WEDecon demultiple, d) Multiples removed by the WEDecon process (Figure 4b – Figure 4c). From Poole et al. (2022).

also noticeable that the gas peg-leg multiples, highlighted by the yellow arrows in Figure 2, have not been captured by the MWD process, which modelled only peg-leg multiples generated by the water bottom. Figure 3 shows the reflectivity derived from the first step of the WEDecon process. Image-domain sparse inversion was used to promote a sharp reflection at the water bottom, ensuring a broadband water bottom multiple prediction (Poole et al., 2021). The reflectivity also captures deeper reflectors, including the gas events observed on the stack sections. Figure 2d shows the multiple prediction from the WEDecon approach. As this was a receiver-side prediction, we can see that the diffraction tail character matches the one observed on the receiver-side MWD prediction, as expected. In contrast to MWD, however, we observe that the gas peg-leg multiple arrival, highlighted by the yellow arrows, has been accurately modelled by this approach. Figures 2e and 2f compare demultiple results using adaptive subtraction for joint source- and receiver-side MWD, with joint source-side MWD and receiver-side WEDecon (proposed by Poole et al., 2021) respectively. We can appreciate that this result has been successful in attenuating the residual gas peg-leg multiple along with some residual low-frequency multiple below the

dipping part of the water bottom (white arrow). Later processing of these data included long-period SRME and internal multiple attenuation to complete the full demultiple sequence.

The next data example comes from a 1650 km² OBN dataset acquired in the Central North Sea with a 50 m × 50 m shot carpet. Prior to demultiple, these data were dealiased and resampled to a 12.5 m × 12.5 m shot carpet. The availability of pressure and vertical geophone measurements allowed estimation of up-going and down-going wavefields which were used as input to up-down deconvolution (Amundsen, 2001). Up-down deconvolution is a very powerful approach, aimed at attenuating the source signature and ghost along with all free-surface multiples in one step. A standard FK implementation of up-down deconvolution was applied in this case, making the assumption that a given down-going plane wave reflects upwards with the same slowness. This assumption may leave residual multiples in the data (Poole et al., 2022). Figure 4a shows a deep-section reverse-time migration (RTM) image of the up-going dataset, heavily contaminated by ringing multiples hanging from every primary arrival. Figure 4b shows the same data after up-down deconvolution, where most of the

multiple energy has been attenuated. However, some residual multiples can be seen at the locations highlighted by the yellow arrows. In this case, WEDecon was applied after up-down deconvolution to further attenuate the residual multiples. For reference, Figure 5a shows the WEDecon reflectivity image derived using raw hydrophone data. This reflectivity image captures the strong water bottom along with other short-period multiple periodicities present in the hydrophone data. Figure 5b shows the WEDecon reflectivity image generated using input data after up-down deconvolution. In this case, the WEDecon reflectivity image using up-down deconvolution data was much weaker than the WEDecon reflectivity image derived using the hydrophone data, as most of the multiples had been removed by the up-down deconvolution process. The reflectivity image highlights the presence of residual periodic multiples from the water bottom as well as shallow gas and channel multiple generators (see yellow arrows in Figure 5b). These multiples were not attenuated by the up-down deconvolution process.
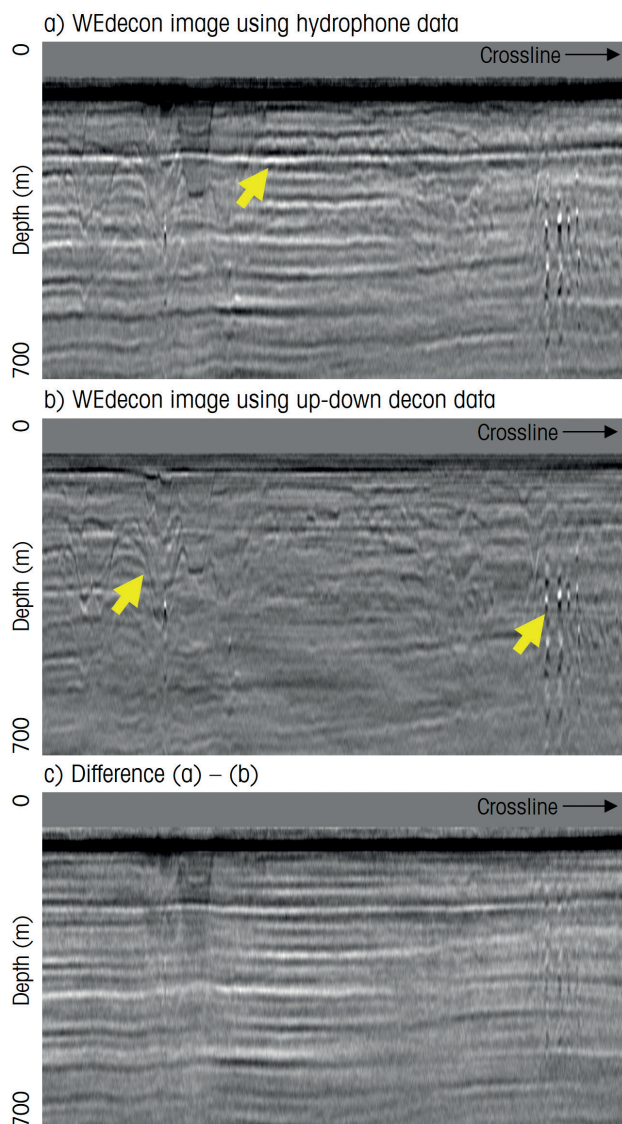

Figure 5 Shallow inline sections for: a) WEDecon reflectivity image using hydrophone data as input, b) WEDecon reflectivity image using data after up-down deconvolution as input, and c) Difference 5a-5b. From Poole et al. (2022).

Figure 5c shows the difference between Figures 5a and 5b. This illustrates the multiple generators with a layer-cake bias that were addressed by the up-down deconvolution process.

The variable effectiveness of multiple attenuation approaches often means that the amplitude level of residual multiples may be variable in space and time, for example depending on the efficiency of adaptive subtraction. This makes residual multiple prediction approaches challenging, as they may easily over-predict or under-predict residual multiples in the data. While the use of adaptive subtraction may adjust for these variations, this is often at the expense of attenuating stronger primary events. In this example the residual multiples after up-down deconvolution (which did not include an adaption step) were sufficiently consistent such that the WEDecon multiple model could be subtracted without adaption. Figure 4c shows the deep RTM image after residual multiple attenuation using WEDecon, with the multiples removed by WEDecon being shown in Figure 4d. As highlighted by the yellow arrows on Figure 4, we observe a significant reduction in the level of multiples by this application of WEDecon.

The final example comes from a 2300 km² high-density land dataset acquired in eastern Algeria (Li et al., 2022). The acquisition used a 30 m × 30 m shot carpet recorded into a 30 m × 210 m receiver spread, resulting in a trace density of approximately 6 million traces/km². Prior to demultiple, these data were processed through denoise, statics correction, and velocity analysis. Surface-related multiple attenuation is particularly challenging for land datasets owing to varying topography and weathering layer properties. Figure 6a shows a deep inline section from the dataset which exhibits high levels of ringing multiples: this is highlighted by the autocorrelation QC which captures the periodic behaviour of these short-period multiples. Figure 6b shows the deep inline section after surface-consistent gapped deconvolution using a 24 ms gap. The approach has attenuated a small amount of low-frequency multiple, but much of the ringing multiple content still contaminates the display. Figure 7a shows a shallow primary image from the dataset, lacking lateral continuity due to missing small reflection angles in the shallow section. Figure 7c shows a depth slice from the primary image, highlighting the acquisition striping responsible for the lack of lateral coherency. Due to the strong acquisition striping, this primary image would be unsuitable for short-period multiple prediction using the method of Pica et al. (2005). Figure 7b shows the shallow section from WEDecon reflectivity imaging. We observe a significant improvement in the lateral continuity of the events on the WEDecon reflectivity image compared to the primary image (Figure 7a). Figure 7d shows a depth slice through this shallow section, exhibiting a significant reduction in the level of acquisition striping compared to the primary depth slice (Figure 7c). Unlike marine data, which benefits from a near-mirror reflection at the free surface, the down-going reflection at the weathering layer will be included as part of the WEDecon reflectivity image. Figure 6c shows the demultiple result using WEDecon, where a significant reduction in the level of ringing multiples can be observed. This is particularly highlighted by the reduced energy levels on the autocorrelation display. On this project, a pass of surface-consistent
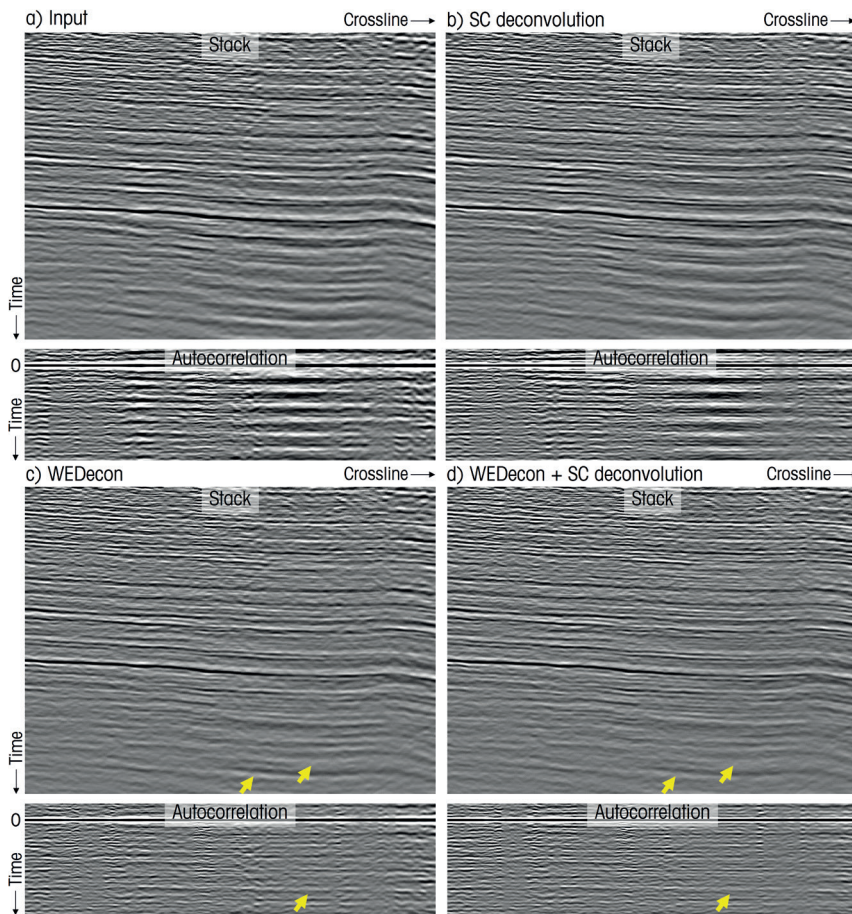
Figure 6 Deep inline sections and autocorrelation displays for: a) Data before demultiple, b) After surface-consistent deconvolution, c) After WEDecon demultiple, and d) After WEDecon demultiple followed by surface-consistent deconvolution.
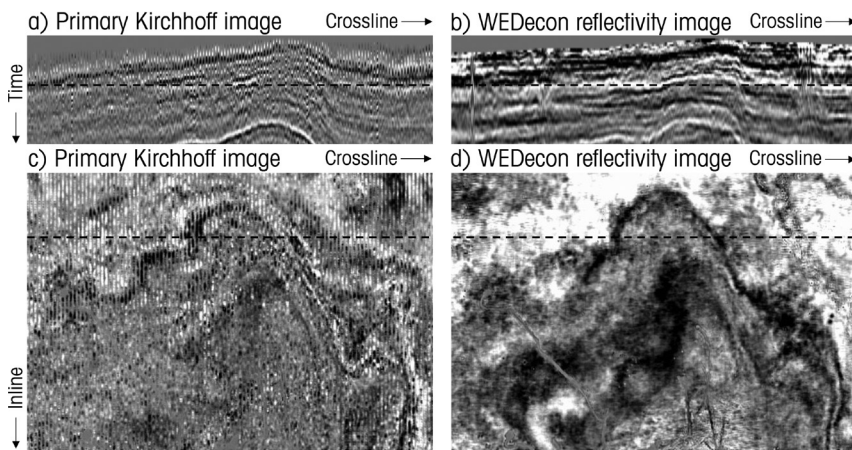

Figure 7 Shallow imaging comparison for: a) Primary imaging inline display, b) WEDecon reflectivity inline display, c) Primary imaging depth slice display, and d) WEDecon reflectivity depth slice display.

deconvolution was applied after WEDecon (Figure 6d), providing an incremental reduction in residual multiple levels (see yellow arrows). There are still some weak residual multiples left in this dataset and we acknowledge that this is a challenging area for further research. Attenuation of interbed multiples would further reduce the multiple content of this data.

Conclusion

Short-period multiple attenuation is often challenging as the multiple generators are typically not sufficiently well recorded as primary events for SRME to be successful. Model-based approaches have traditionally been used to circumvent this problem but may only model multiples generated by key events, such as the water bottom. Deconvolution-based alternatives offer the possibility to model multiples from more short-period multiple generators, but, in practice, many acquisition geometries are not well suited to higher-dimensional deconvolution implementations. We have discussed a wave-equation deconvolution approach (WEDecon) which derives its prediction operator in the image domain. The image is then used to predict multiples, which are removed from the data. We highlight the flexibility of WEDecon using data examples from towed-streamer, OBN, and land geometries. The WEDecon approach has been successful at significantly reducing levels of residual multiples present in all these data types. We acknowledge, however, that short-period multiple attenuation is still a challenging topic and further work is necessary in this area.

References

Amundsen, L. [2001]. Elimination of free-surface related multiples without the need of the source wavelet. *Geophysics*, **66**, 327-341.

Berkhout, A.J. and Verschuur, D.J. [1997]. Estimation of multiple scattering by iterative inversion, Part I: theoretical consideration. *Geophysics*, **62**, 1586-1595.

Biersteker, J. [2001]. MAGIC: Shell's surface multiple attenuation technique. 71st Annual International Meeting, SEG, Expanded Abstracts.

Biondi, B.L. [2006]. 3D seismic imaging. *Investigations in Geophysics*, SEG publication.

Cooper, J., Poole, G., Wombell, R. and Wang, P. [2015]. Recursive model-based water-layer demultiple. 77th EAGE Conference and Exhibition, Expanded Abstracts.

Li, B., Miorali, M., Mills, K. and Poole, G. [2022]. Least-squares multiple imaging for 3D surface-related multiple elimination on land data.

Paper presented at the International Petroleum Technology Conference, Riyadh, Saudi Arabia, paper number IPTC-21935-EA.

Pica, A., Poulain, G., David, B., Magesan, M., Baldock, S., Weisser, T., Hugonnet, P. and Herrmann, P. [2005]. 3D surface-related multiple modeling, principles and results. 75th Annual International Meeting, SEG, Expanded Abstracts.

Poole, G. [2019]. Shallow water surface related multiple attenuation using multi-sailline 3D deconvolution imaging. 81st EAGE Conference and Exhibition, Extended Abstracts, Tu R1 5.

Poole, G., Moore, H., Blaszczak, E., Kerrison, H., Keynejad, S., Taboga, A. and Chappell, M. [2021]. Sparse wave-equation deconvolution imaging for improved shallow water demultiple. 83rd EAGE Conference and Exhibition, Extended Abstracts.

Poole, G., Jin, Z., Irving, A., and Refaat, R. [2022]. Adaption-free OBN demultiple using up-down deconvolution and wave-equation deconvolution. 84th EAGE Conference and Exhibition, Extended Abstracts.

Wang, P., Jin, H., Xu, S. and Zhang, Y. [2011]. Model-based water-layer demultiple. 81st Annual International Meeting, SEG, Expanded Abstracts.

Wiggins, W. [1988]. Attenuation of complex water-bottom multiples by wave-equation-based prediction and subtraction. *Geophysics*, **53**, 1527-1539.